AIMS Biophysics, 4(4): 528-542.
DOI: 10.3934/biophy.2017.4.528
Received: 24 July 2017
Accepted: 22 August 2017
Published: 29 August 2017

http://www.aimspress.com/journal/biophysics

Research article

Lipid phase separation in the presence of hydrocarbons in giant unilamellar vesicles

Rianne Bartelds, Jonathan Barnoud, Arnold J. Boersma, Siewert J. Marrink, and Bert Poolman *

Groningen Biomolecular Sciences and Biotechnology Institute and Zernike Institute for Advanced Materials, University of Groningen, Nijenborgh 7, 9747 AG Groningen, The Netherlands

*** Correspondence:** Email: b.poolman@rug.nl; Tel: +31-50-3634190.

Abstract: Hydrophobic hydrocarbons are absorbed by cell membranes. The effects of hydrocarbons on biological membranes have been studied extensively, but less is known how these compounds affect lipid phase separation. Here, we show that pyrene and pyrene-like hydrocarbons can dissipate lipid domains in phase separating giant unilamellar vesicles at room temperature. In contrast, related aromatic compounds left the phase separation intact, even at high concentration. We hypothesize that this behavior is because pyrene and related compounds lack preference for either the liquid-ordered (L_o) or liquid-disordered (L_d) phase, while larger molecules prefer L_o, and smaller, less hydrophobic molecules prefer L_d. In addition, our data suggest that localization in the bilayer (depth) and the shape of the molecules might contribute to the effects of the aromatic compounds. Localization and shape of pyrene and related compounds are similar to cholesterol and therefore these molecules could behave as such.

Keywords: biological membranes; lipid phase separation; unilamellar vesicles; hydrocarbons; membrane partitioning; polycyclic aromatic hydrocarbons; fluorescence microscopy

1. Introduction

The plasma membrane is the main permeability barrier of the cell and consists of hundreds to thousands of different lipid species in addition to a wide range of proteins that allow the cell to sense the environment and transport specific molecules in and out of the cell. The lipids of the membrane

are not randomly distributed but can form distinct domains, often referred to as lipid rafts, and associate with specific proteins [1,2,3]. Rafts are associated with specific membrane proteins, thereby affecting signaling and protein trafficking in the membrane as summarized by Levental and Veatch [4].

Hydrocarbons affect the membrane properties as they interfere with the interaction of proteins with their neighboring lipids. Alternatively, the hydrocarbons can bind to hydrophobic pockets or surfaces of proteins and thereby influence their activity. Local anesthetics exert their effects by e.g. decreasing the miscibility temperature of lipids as shown in giant plasma membrane vesicles [5], thereby increasing the membrane fluidity. In another study, hydrophobic phytochemicals were shown to perturb the phospholipid bilayer and the proteins embedded in there [6]. In general, hydrocarbons alter membrane properties such as membrane thickness, head group hydration and fluidity, all of which can affect membrane proteins [7].

The toxicity of hydrocarbons and other molecules is frequently related to the hydrophobicity of the compounds. A measure for hydrophobicity is the log*P* value, the partitioning of a molecule over octanol and water. The more hydrophobic the compound (as indicated by a higher, positive log*P* value), the more it partitions in octanol and accordingly the higher the concentration in the membrane [8,9]. For instance, 20 mg of petroleum hydrocarbons per gram lipids have been found in oysters [10] and 93 μg/g lipid in maple leaves [11]. Organisms respond to hydrophobic pollutants by changing their membrane composition, by degrading PAHs and by expressing efflux pumps to expel the molecules from the membrane [7,12,13]. It has been shown that *Escherichia coli* and *Ralstonia eutropha* cells change their lipid saturation to make up for the fluidizing or ordering effects of the pollutant when exposed to phenol or biphenyl [14,15].

Aliphatic hydrocarbons localize in the central part of the bilayer [16,17]. Molecular dynamics (MD) simulations confirm experimental studies and found that aliphatic hexane [18] and ethane [19] reside in the hydrophobic center of the bilayer. As a general rule, amphipathic molecules partition near the bilayer interface, while more hydrophobic molecules reside near the bilayer center. In the center of the bilayer, aliphatic hydrocarbons interact with the acyl chains of the phospholipids and increase the area occupied by a phospholipid [20]. This localization prevents Van der Waals interactions between neighboring lipids, thereby fluidizing the membrane. In contrast, long chain alkanes interdigitate between the leaflets, thereby increasing the overall degree of ordering in the membrane [16].

The effects of cyclic hydrocarbons on biological membranes were studied extensively in the early 90's [8], reviewed in Sikkema et al., 1995. It was found that the partitioning in the membrane of cyclic hydrocarbons scales linearly with the log*P* values of the molecules and they expand the membrane [7]. In membrane vesicles derived from *Escherichia coli* cells the hydrocarbons thicken the bilayer and increased the membrane fluidity. In addition, the membranes became more permeable to protons, and, accordingly, it became more difficult to maintain a proton motive force. It was then concluded that global deformation of the membrane likely accounts for the toxicity effects.

Polycyclic aromatic hydrocarbons (PAHs) are found as pollutants in the environment, mainly as a result of incomplete combustion. PAHs are very stable and persistent once formed, and they may accumulate in the center of lipid bilayers [7]. Such localization was found for the aromatic benzene [19,21,22] and pyrene [23,24,25]. Simulation data on the interaction of small, aromatic molecules are described in [26]. The toxicity of PAHs in eukaryotes is dual and relates in part to their hydrophobicity. First, these molecules accumulate in lipid membranes and affect membrane function. Second, to remove these compounds from the cell membrane, the PAHs are chemically

activated by epoxidation, but the modified compounds can also react with other molecules in the cell such as DNA. Depending on where the PAH epoxidation takes place, these metabolites are carcinogenic [27].

Biological membranes are heterogeneous and consist of domains [28] that are on the nanometer scale and short-lived [29], making it a challenge to study their properties. We use giant unilamellar vesicles (GUVs) with detergent-resistant membrane domains (DRMs) as model systems to study mixing effects of hydrocarbons on lipid domain formation. Phase-separating GUVs can be made from a minimum of three components: typically a saturated lipid, an unsaturated lipid and a sterol. At the right ratio of lipids, the GUVs have a liquid-ordered (L_o) phase, enriched in the saturated lipid and cholesterol, and a liquid-disordered (L_d) phase, mainly consisting of the unsaturated lipid [30,31]. Detergent-resistant membranes (DRMs) derived from phase-separating vesicles are closely related to the L_o domains. Lipids associated with the L_o phase were enriched in DRMs [32], and the DRM fraction can only be obtained from vesicles that are phase-separating or in the L_o phase [33,34]. In addition, the L_o phase of phase-separating supported bilayers was found detergent resistant [35]. These model membranes mimic the behavior of natural lipid mixtures [36–39].

In previous work, the aromatic L_o preferring dye naphtopyrene was found to perturb the membrane around the miscibility transition temperature at concentrations of 0.3 mol% [40]. A recent molecular dynamics study by Barnoud and coworkers [41] indicated a difference between the effects of aromatic and aliphatic compounds. While aliphatic compounds induced mixing of a phase-separating membrane, aromatic hydrocarbons stabilized the phase separation.

To better understand the toxicity of PAHs in eukaryotic cells, we determined their effects (Figure 1) on the lipid phase separation in GUVs. We benchmarked the effects of aromatic compounds of varying size against unsubstituted aliphatic compounds as the molecules are expected to interact differently with lipids and are expected to partition in different places of the lipid bilayer. Indeed, we find that the effects on phase separation are highly dependent on the partitioning behavior of the hydrocarbons. Furthermore, we find differences for membranes with DPPC or SSM as the saturated lipid component, indicating that subtle variations in the membrane lipid composition can have major impact when membrane-active compounds are present in the environment. The lipid mixing effect of PAHs and differences between experiments and simulations are discussed and put in perspective.

2. Materials and Methods

2.1. Materials

DPPC, SSM, DOPC and cholesterol were purchased from Avanti Polar Lipids. ATTO 550 DOPE and ATTO 655 DOPE were used as fluorescent probes to visualize the L_d phase and obtained from ATTO-Tec. The dyes are both hydrophilic but differ in their charge (cationic versus zwitterionic). We used both dyes to minimize the possibility of artifacts due to interactions between dye and lipids or and dye and PAHs. The hydrocarbons naphthalene, tetracene, chrysene, pyrene, perylene, triphenylene, coronene, octane and hexadecane were purchased from Sigma-Aldrich, and of fluorescence grade when available. Corannulene was purchased from TCI Europe. Structures of the hydrocarbons used in this study are presented in Figure 1 and their properties are listed in Table 1.

Table 1. Properties of hydrocarbons used in this study.

Compound	Molecular formula	Mw (g/mol)	Boiling point (℃)	log *P*[c]	XLog *P3*[d]	Absorption max (nm)	Absorption max (nm)[a]	Em max (nm)[a]
Naphthalene	$C_{10}H_8$	128.17052	218	3.3/3.35	3.3	221, 275.5, 286, 311	220, 275, 286, 311	322, 334
Phenanthrene	$C_{14}H_{10}$	178.2292	340	4.46	4.5	210, 219, 242, 251, 273.5, 281, 292.5, 308.5, 314, 322.5, 329.5, 337, 345		
Tetracene	$C_{18}H_{12}$	228.28788	450[b]	5.76–6.02[b]	5.9			
Chrysene	$C_{18}H_{12}$	228.28788	448	5.73/5.9	5.7	222, 258, 268, 295, 353, 361, 344, 320		
Pyrene	$C_{16}H_{10}$	202.2506	404/399	4.88	4.9	273, 306, 320, 335	241, 273, 335	349, 381
Triphenylene	$C_{18}H_{12}$	228.28788	425[b]	4.83–5.84[b]	4.9			
Benzo(e)pyrene	$C_{20}H_{12}$	252.30928	310–312	6.44	6.4			
Perylene	$C_{20}H_{12}$	252.30928	350–400 (sublimes)	5.82	5.8	245, 251, 368, 387, 406, 434	387, 408, 436	436, 463, 497
Corannulene	$C_{20}H_{10}$	250.2934			6			
Coronene	$C_{24}H_{12}$	300.35208	525[b]	5.4–8.2[b]	7.2			
Octane	C_8H_{18}	114.22852	126	5.18	3.9			
Hexadecane	$C_{16}H_{34}$	226.44116	286.5	8.25 (est)	8.3			

Data from Pubchem database, except [a]http://omlc.org/spectra/PhotochemCAD/index.html; [b]Mackay D, Shiu WY, Ma KC, et al. (2006) *Handbook of Physical-Chemical Properties and Environmental Fate for Organic Chemicals*, 2 Eds., CRC Press. [c]log*P* = log ($[solute]_{octanol}/[solute]_{water}$); [d]Xlog*P3* = a calculated log*P* value [57].

2.2. GUV formation

GUVs were prepared by electroformation as described previously [31]. Lipid mixtures consisting of DPPC/DOPC/cholesterol or SSM/DOPC/cholesterol in a 4:3:3 ratio (all in chloroform/methanol 9:1) were prepared out of 5 mM stocks. To visualize the GUVs, 0.1% ATTO 550 DOPE or ATTO 655 DOPE was added. 15 μL of the lipid mixture was placed on a conductive indium tin oxide (ITO) coated glass plate. Solvents were removed by placing the coverslips with lipids in a vacuum desiccator for 1 h. A rubber ring (Ø15 mm) was placed around the lipids with grease. After preheating the glass plates and water to 50 ℃, the ITO-plate containing the lipids was placed on the Vesicle Prep Pro (Nanion Technologies). 200 μL water was added and the chamber was closed by putting a second ITO plate on top. A voltage of 1.1 V was applied for 1 h, at 10 Hz

and 50 ℃ to form the GUVs. Afterwards, the chamber was disassembled and the GUVs were studied by confocal microscopy.

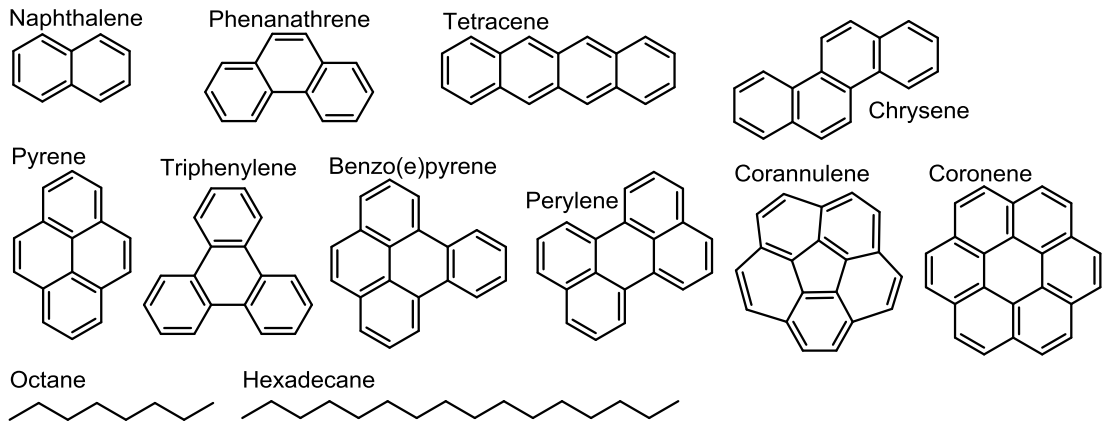

Figure 1. Structures of the compounds used in this study.

2.3. Addition of hydrocarbons

Hydrocarbons dissolved in chloroform/methanol 9:1 or when indicated in dimethylformamide (DMF) were added to the lipid mixture or to GUVs. As solvent control, the maximal solvent concentration was taken as extra condition. To study the effect of hydrocarbons, the compounds dissolved in chloroform/methanol 1:1 were added to the lipid mixture. The GUVs formed were imaged on a commercial LSM 710 confocal microscope (Zeiss), using a 40× C-Apochromat Corr M27 with NA 1.2 water immersion objective. ATTO 550 DOPE was excited with a 543 nm HeNe laser, ATTO 655 DOPE with a 633 nm HeNe laser. Perylene was excited with a 405 nm diode laser.

2.4. Data analysis

To quantify the effect of hydrocarbons on phase separation, the partitioning of the dyes over the L_o and L_d phases was used and reported as pL_o/L_d ratio. This ratio is equivalent to the partitioning coefficient (K_p) that was used by Levental and coworkers [1]. A 5 pixel wide line was drawn through the middle of a GUV to avoid polarization effects, as shown in Figure 2. The maxima of both peaks were determined and the pL_o/L_d was calculated. At least 50 GUVs per condition for each experiment were analysed.

2.5. Detergent-resistant membranes (DRMs)

To probe the partitioning of the PAHs, DRMs were prepared from multilamellar vesicles as previously described [42], with slight modifications. Briefly, multilamellar vesicles were formed by thin film hydration. The appropriate amount of lipids, dissolved in chloroform/methanol 9:1, were mixed and solvents were evaporated by rotary evaporation. Next, the lipid film was hydrated in 10 mM Tris-HCl, 150 mM NaCl, pH 7.4 by repeated vortexing at 60 ℃; the final lipid concentration was made 1 mM. To isolate DRMs, ice cold Triton X-100 was added to chilled MLVs in a 1:1 mol

Triton X-100 to lipid ratio. These conditions were chosen to observe similar perylene partitioning in the vesicles with DRMs as in the GUVs with L_d and L_o phases (see Figure 5). After 30 minutes of incubation on ice, the DRMs were obtained by ultracentrifugation at 227,000 g for 1 h at 4 ℃. The supernatant was removed and the pellet resuspended in the same volume of Tris/NaCl buffer. Fluorescence of the pellet and the supernatant was measured on a fluorimeter (Jasco FP-8300).

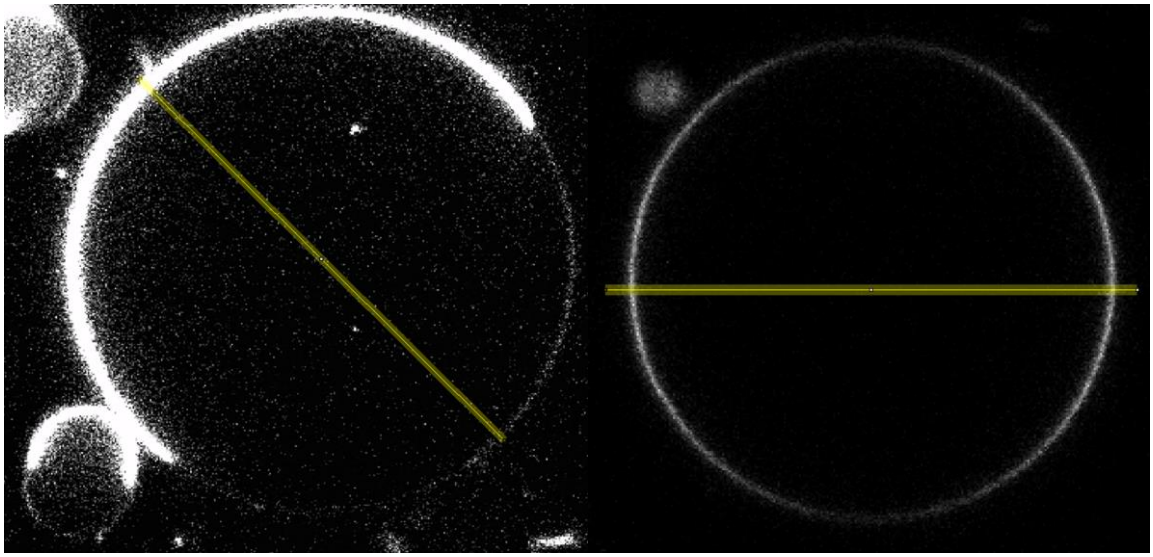

Figure 2. Fluorescent quantification of pL_o/L_d. Partition coefficients of the dyes were quantified by a 5 pixel width line scan through the domains. Only GUVs with both domains in the middle (as in the left picture) were analyzed. When no phase separation was visible, a line was drawn from left to right through the middle of the GUV (as in the right panel).

3. Results

3.1. Pyrene and related compounds prevent phase separation

Pyrene, triphenylene and benzo(e)pyrene prevented phase separation in GUV, composed of DPPC, DOPC and cholesterol when added to the lipid mixture in a 1 to 1 molar ratio (Figure 3A). The other tested aromatic hydrocarbons, i.e. naphthalene, phenanthrene, tetracene, chrysene, perylene, coronene and corannulene, retained phase separation, even at such high concentrations. Also for the aliphatic octane and hexadecane, no effect on phase separation was observed. The majority of the GUVs are either phase separating (indicated by a pL_o/L_d close to 0) or uniform (indicated by a pL_o/L_d close to 1). In the GUVs analyzed, few vesicles displayed an intermediate appearance between phase separation and one phase (where phase separation is maintained, but the dye partitioning is not as black and white as in the example shown in Figure 2), which is indicated by a pL_o/L_d value between 0.2 and 0.8 (Figure 3B).

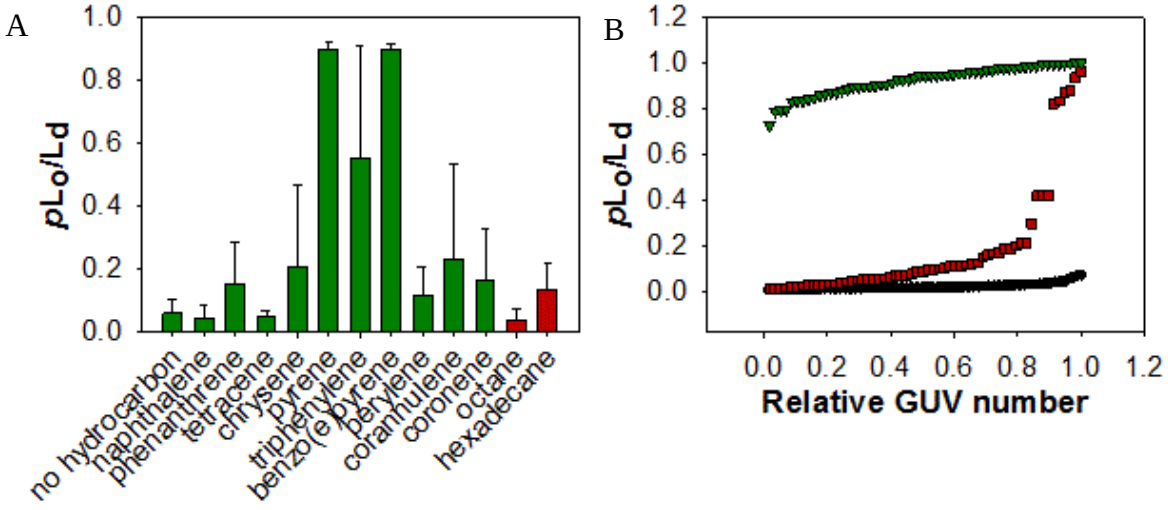

Figure 3. Pyrene and related molecules prevent phase separation in GUVs composed of DPPC/DOPC/cholesterol. A: GUVs composed of DPPC/DOPC/cholesterol at a ratio of 4:3:3 and the solutes dissolved in chloroform/methanol were used. The pL_o/L_d ratio was determined using ATTO 550 DOPE as probe and the hydrocarbons were added to the lipid mixture prior to GUV formation. The error reflects variations in different GUV preparations. All compounds are present in a 1 to 1 mol ratio with the lipids. In green: aromatic hydrocarbons; in red: aliphatic hydrocarbons. B: Distribution plot of one representative experiment, for three conditions. pL_o/L_d values of individual GUVs (indicated by a symbol) are ordered from 0 (lowest pL_o/L_d ratio measured for that condition) to 1 (highest pL_o/L_d ratio measured) according to the their pL_o/L_d ratio; the pL_o/L_d ratios are plotted against the GUV number. We normalized the values of the x-axis, because the GUV numbers are not the same for the three conditions. Black line: 2.5 mol% pyrene; red line: 10 mol% pyrene; green line: 50 mol% pyrene. In A, values are mean ± standard deviation of at least three independent experiments (biological replicates) except for naphthalene, tetracene, coronene, octane and hexadecane (n = 2), and triphenylene and corannulene (n = 4).

Irrespective of whether the hydrocarbon was introduced prior to or after GUV formation, pyrene dissipated phase separation in the GUVs (Figure S1A). Adding pyrene dissolved in DMF to phase-separating GUVs increased the pL_o/L_d from 0.07 to 0.86. Various fluorescent probes, used to visualize membranes, have been shown to alter the miscibility temperature of membranes [40,43,44,45]. Therefore, to rule out possible effects of the cationic membrane probe (ATTO 550 DOPE), the experiments were repeated with the zwitterionic ATTO 655 DOPE but the results were similar (see Figure S1B).

3.2. Phase separation only disappears at high PAH to lipid ratios and is lipid composition dependent

To study if the mixing effect of pyrene is lipid specific, the effect of pyrene was also studied in GUVs prepared from SSM/DOPC/cholesterol (Figure 4). At similar pyrene to lipid ratios, phase separation was maintained in SSM/DOPC/cholesterol GUVs but not in vesicles prepared from

DPPC/DOPC/cholesterol. These results are consistent with previous measurements [46–49], which showed that the interaction between SSM and cholesterol is stronger than the interaction between DPPC and cholesterol. Accordingly, the impact of pyrene and most likely other PAHs on phase separation is clear when DPPC is present, in contrast with the sphingolipid.

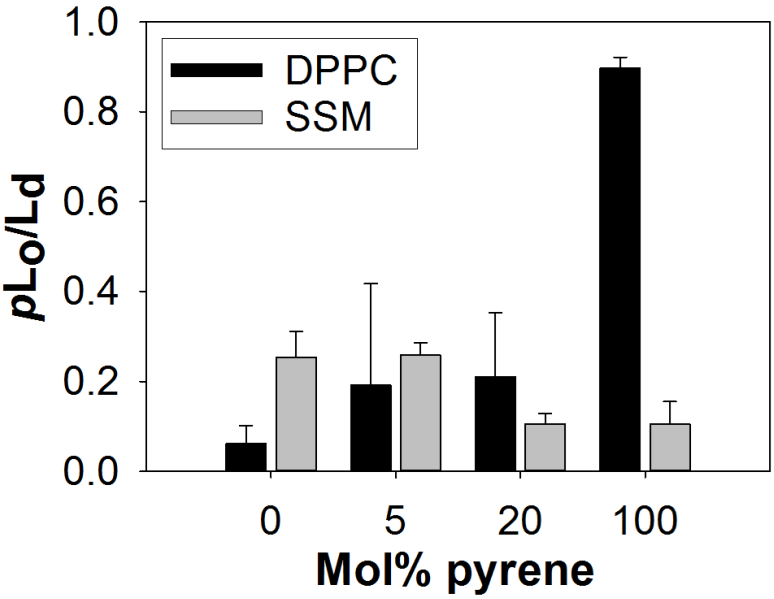

Figure 4. Phase separation disappears at high PAH to lipid ratios and is dependent on lipid composition. The pL_o/L_d ratio estimated from the ATTO 550 DPPE partitioning in GUVs composed of DPPC/DOPC/cholesterol or SSM/DOPC/cholesterol (mol ratios of 4:3:3) with and without the indicated mol% of pyrene. Values are mean ± standard deviation of at least two independent experiments.

3.3. PAH localization depends on hydrophobicity and shape

The localization of PAHs was studied in DRMs, since these resemble the L_o phase and PAH partitioning can be determined spectroscopically. Here, we observe that the more hydrophobic the compound (as indicated by the log*P* values; Table 1) the higher the partitioning in the DRM (Figure 5). Small PAHs such as naphthalene and phenanthrene have a preference for the L_d phase (indicated by the $I_{pellet}/I_{supernatant} < 1$), while the larger compounds tetracene and coronene reside mainly in the L_o phase ($I_{pellet}/I_{supernatant} > 1$). Strikingly, with the exception of corannulene, the three compounds that prevent phase separation in GUVs equally partitioned in both phases ($I_{pellet}/I_{supernatant} \approx 1$). To check if the partitioning of hydrocarbons in DRMs is comparable to partitioning in GUVs, the localization of perylene was tested by an independent method. Perylene absorbs blue light and has a fluorescence emission maximum at 436 nm and can therefore be followed by confocal microscopy. The fluorescence-based analyses in GUVs were compared to the results from DRMs (Figure 6), and indeed a similar localization was found.

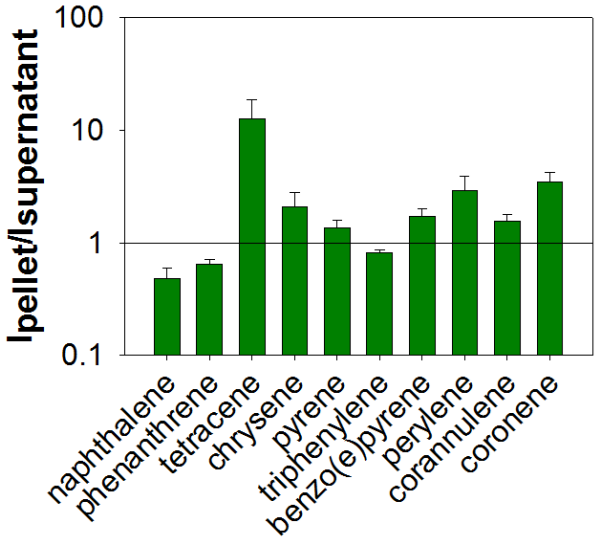

Figure 5. PAH localization in detergent resistant membranes. The $I_{pellet}/I_{supernatant}$ was calculated from the fluorescence of the pellet (DRM) and the fluorescence of the supernatant at the maximum emission. All compounds were present at 2 mol% hydrocarbon-to-lipid ratio to prevent excimer formation. Values are mean ± standard deviation of at least two independent experiments.

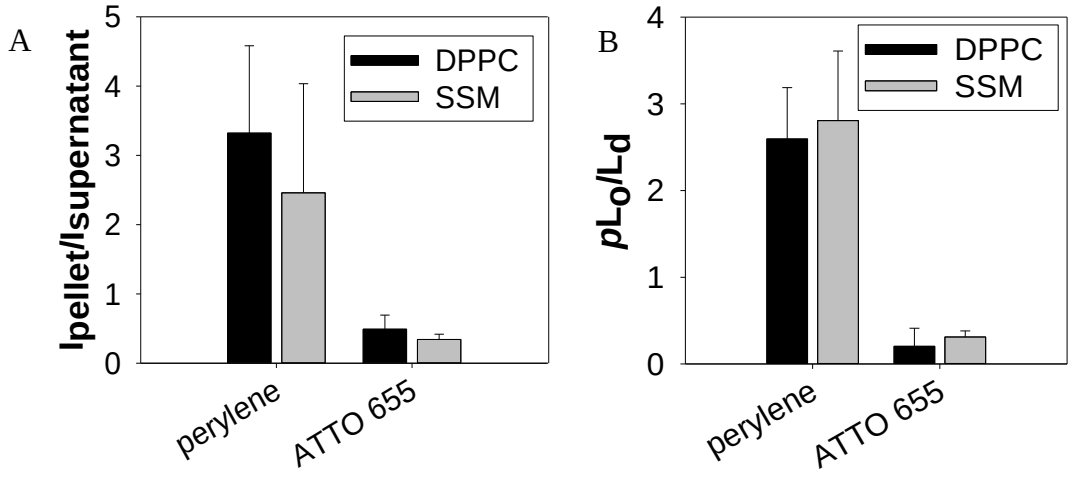

Figure 6. Perylene localization in GUVs and DRMs. A: the pL_o/L_d ratio of perylene in both DPPC/DOPC/cholesterol and SSM/DOPC/cholesterol GUVs (mol ratios of 4:3:3) GUVs; 2 mol% perylene was added to the lipid mixture prior to GUV formation. B: the $I_{pellet}/I_{supernatant}$ of perylene were determined in multilamellar vesicles of the aforementioned lipid mixtures with 2 mol% perylene. Values are mean ± standard deviation of at least two independent experiments.

4. Conclusions

We find that at room temperature high concentrations of the hydrocarbons naphthalene, phenanthrene, tetracene, chrysene, perylene, corannulene, corulene, octane and hexadecane have a

rather small effect on lipid phase separation in vesicles composed of DPPC, DOPC and cholesterol. Differences in phase separation are not visible even when hydrocarbons are present in amounts stoichiometric with the membrane lipids. Pyrene, benzo(e)pyrene and triphenylene form an exception, in that these compounds induce lipid mixing in phase-separating GUVs containing DPPC but not when DPPC is replaced by SSM. The specific effect of pyrene-like compounds is likely due to their partitioning in both the L_o and L_d phase, which is explained by the shape and hydrophobicity of the hydrocarbon.

According to MD simulations and fluorescence quenching experiments, pyrene is localized predominantly in the highly ordered upper region of the acyl chains of POPC/DPPC membranes [23,24], at a similar position as cholesterol [50]. Pyrene does not reach as deep as cholesterol into the bilayer, thereby leaving space below the pyrene molecule and the center of the membrane. The tails of unsaturated lipids such as DOPC can occupy this space [50]. Hexadecane is located in a similar fashion as pyrene according to X-ray diffraction data [16]. On the contrary, octane is localized between the two leaflets in the same study. To the best of our knowledge, for the other compounds used in this study no localization data is available.

Besides its position in the upper region of the acyl chains, pyrene has more in common with cholesterol. In MD simulations, pyrene had an ordering effect on neighboring DPPC molecules in the fluid phase, while it has a disordering effect on the same molecules in the gel phase [21]. This is similar to the effect of cholesterol in DPPC membranes [51]. In addition, pyrene has a diamond shape and occupies the equivalent geometric volume of the membrane [50]. Compared to e.g. tetracene or chrysene, more space is available below the pyrene molecule. If indeed pyrene behaves as cholesterol, the membrane becomes saturated and differences between the L_o and the L_d phase become smaller. Eventually, both phases mix as seen in ternary lipid mixtures (e.g. DPPC, DOPC, and cholesterol [30]) that contain over 40% cholesterol and this is what we find here with pyrene.

Large PAHs have a preference for the L_o phase [39], while benzene and fullerene end up in the L_d phase of phase-separating bilayers in MD simulations [41]. This is in agreement with the localization of PAHs in DRMs measured here. The large rigid compounds induce order by forcing the acyl chains to arrange themselves around the molecule, which occurs with an entropic penalty [24]. In the already more ordered L_o phase, the costs are lower than in less ordered L_d phase, hence the preference of these compounds for L_o.

The exact localization of pyrene in phase-separating membranes has not been reported but can be deduced from literature using similar compounds. The partitioning of aromatic dyes is not only dependent of their hydrophobicity but also of their size and shape. Relatively small dyes such as perylene and rubicene were found in both the L_o and L_d phase of GUVs composed of brain SM, DOPC and cholesterol, larger dyes such as terrylene and naphthopyrene partitioned in the L_o phase [52]. Naphthopyrene also partitions into the L_o phase of GUVs composed of DPPC/DOPC/cholesterol [53]. However, the dye phase preference varies between lipid mixtures. For example perylene has L_o preference in GUVs composed of egg SM (mainly consisting of short chain (C16) saturated SM), DOPC and cholesterol [54], while in brain SM (consisting of longer chain SMs (C18 to C24) and 20% unsaturated chains), DOPC and cholesterol GUVs perylene does not have a preference for any of the phases [52]. These studies indicate that the more hydrophobic the dye, the more likely it is that it localizes in the L_o phase, but only few very hydrophobic compounds end up in that L_o phase and it depends on the lipid mixture used how a dye is distributed across both phases (a L_o phase in one lipid mixture is different from a L_o phase in another lipid mixture).

The dissipation of phase separation with pyrene and related compounds was only observed in vesicles containing DPPC. Although it is often claimed that DPPC and SM act similar in phase separating mixtures, the strength of the interaction of these lipids with e.g. cholesterol is different. The preference of cholesterol for SM is explained by the presence of the N-linked acyl chain. The amide of SM can act as hydrogen bond donor and acceptor with the hydroxyl moiety of the cholesterol [55]. Due to the stronger interactions between cholesterol and SSM, pyrene most likely cannot perturb phase separation, i.e. under conditions that it does in GUVs with DPPC instead of SSM. Other studies have shown different partitioning of the dye DiI C18:0, depending on the saturated lipid component. The DiI C18:0 dye partitions into the L_d phase of brain SM-containing GUVs and in the L_o phase in distearoylphosphatidylcholine-containing GUVs [52]. The authors explain this effect due to the preferential interaction of cholesterol with SM (excluding the DiI C18:0 from this phase) compared to saturated phospholipids. This is also confirmed by ^{2}H-NMR [46,49], solid-state NMR combined with DSC [48] and DPH anisotropy measurements, using a fluorescent cholesterol analogue [47].

Aliphatic hydrocarbons had no effect on phase separation in GUVs composed of DPPC, DOPC and cholesterol, analyzed at room temperature. This is in contrast to previous MD simulations, where these molecules act as lineactant and decrease phase separation [41]. We attribute the differences in the experiments and simulations to either differences in lipid composition (the simulation studies use polyunsaturated lipids to increase the phase separation) or setup (small periodic lamellar patches with a surface in the order of 520 nm^2 in case of the MD simulations versus GUVs in the experiments). An older study found that the aromatic benzene and toluene increase membrane fluidity, but the aliphatic cyclohexane and hexane did not alter membrane fluidity as measured by pyrene excimer formation [56]. This is in line with the results presented here, where only some aromatic compounds alter phase separation.

In conclusion, we show that at room temperature hydrocarbons have a distinct effect on lipid phase separation, and the effect is dependent on the strength of the interaction of cholesterol with the saturated lipid component. Pyrene and pyrene-like compounds dissipate phase separation in mixtures containing DPPC as saturated lipid component but not in GUVs containing SSM instead of DPPC. We speculate that pyrene and related compounds act as cholesterol, thereby decreasing the difference between the L_o and L_d phase and eventually leading to domain mixing. Furthermore, PAHs larger than pyrene-like compounds prefer L_o, whereas smaller ones partition in L_d.

Acknowledgements

This work was supported by the Netherlands Organisation for Scientific Research (NWO): Chem-Them grant 728.011.202. Prof. Gerard Roelfes and Hugo van Oosterhout are kindly acknowledged for fruitful discussions.

Conflict of Interest.

All authors declare no conflicts of interest in this paper.

References

1. Levental I, Lingwood D, Grzybek M, et al. (2010) Palmitoylation regulates raft affinity for the majority of integral raft proteins. *Proc Natl Acad Sci* 107: 22050–22054.
2. Bryant DM, Mostov KE (2008) From cells to organs: building polarized tissue. *Nat Rev Mol Cell Biol* 9: 887–901.
3. Hashimoto-Tane A, Yokosuka T, Ishihara C, et al. (2010) T-cell receptor microclusters critical for T-cell activation are formed independently of lipid raft clustering. *Mol Cell Biol* 30: 3421–3429.
4. Levental I, Veatch SL (2016) The continuing mystery of lipid rafts. *J Mol Biol* 428: 4749–4764.
5. Gray E, Karslake J, Machta B, et al. (2013) Liquid general anesthetics lower critical temperatures in plasma membrane vesicles. *Biophys J* 105: 2751–2759.
6. Ingólfsson HI, Thakur P, Herold KF, et al. (2014) Phytochemicals perturb membranes and promiscuously alter protein function. *ACS Chem Biol* 9: 1788–1798.
7. Sikkema J, De Bont JA, Poolman B (1995) Mechanisms of membrane toxicity of hydrocarbons. *Microbiol Rev* 59: 201–222.
8. Sikkema J, De Bont JAM, Poolman B (1994) Interactions of cyclic hydrocarbons with biological membranes. *J Biol Chem* 269: 8022–8028.
9. McKarns SC, Hansch C, Caldwell WS, et al. (1997) Correlation between hydrophobicity of short-chain aliphatic alcohols and their ability to alter plasma membrane integrity. *Fundam Appl Toxicol* 36: 62–70.
10. Stegeman JJ, Teal JM (1973) Accumulation, release and retention of petroleum hydrocarbons by the oyster Crassostrea virginica. *Mar Biol* 22: 37–44.
11. Wagrowski DM, Hites RA (1996) Polycyclic aromatic hydrocarbon accumulation in urban, suburban, and rural vegetation. *Environ Sci Technol* 31: 279–282.
12. Hearn EM, Dennis JJ, Gray MR, et al. (2003) Identification and characterization of the emhABC efflux system for polycyclic aromatic hydrocarbons in Pseudomonas fluorescens cLP6a. *J Bacteriol* 185: 6233–6240.
13. Bugg T, Foght JM, Pickard MA, et al. (2000) Uptake and active efflux of polycyclic aromatic hydrocarbons by Pseudomonas uptake and active efflux of polycyclic aromatic hydrocarbons by Pseudomonas fluorescens LP6a. *Appl Environ Microbiol* 66: 5387–5392.
14. Keweloh H, Diefenbach R, Rehm HJ (1991) Increase of phenol tolerance of Escherichia coli by alterations of the fatty acid composition of the membrane lipids. *Arch Microbiol* 157: 49–53.
15. Kim IS, Lee H, Trevors JT (2001) Effects of 2,2',5,5'-tetrachlorobiphenyl and biphenyl on cell membranes of Ralstonia eutropha H850. *FEMS Microbiol Lett* 200: 17–24.
16. McIntosh TJ, Simon SA, MacDonald RC (1980) The organization of n-alkanes in lipid bilayers. *BBA-Biomembranes* 597: 445–463.
17. White SH, King GI, Cain JE (1981) Location of hexane in lipid bilayers determined by neutron diffraction. *Nature* 290: 161–163.
18. MacCallum JL, Tieleman DP (2006) Computer simulation of the distribution of hexane in a lipid bilayer: Spatially resolved free energy, entropy, and enthalpy profiles. *J Am Chem Soc* 128: 125–130.
19. Bemporad D, Essex JW, Luttmann C (2004) Permeation of small molecules through a lipid bilayer: A computer simulation study. *J Phys Chem B* 108: 4875–4884.

20. Cornell BA, Separovic F (1983) Membrane thickness and acyl chain length. *BBA-Biomembranes* 733: 189–193.
21. Norman KE, Nymeyer H (2006) Indole localization in lipid membranes revealed by molecular simulation. *Biophys J* 91: 2046–2054.
22. Bassolino-klimas D, Alper HE, Stouch TR (1995) Mechanism of solute diffusion through lipid bilayer membranes by molecular dynamics simulation. *J Am Chem Soc* 117: 4118–4129.
23. Čurdová J, Čapková P, Plášek J, et al. (2007) Free pyrene probes in gel and fluid membranes: Perspective through atomistic simulations. *J Phys Chem B* 111: 3640–3650.
24. Hoff B, Strandberg E, Ulrich AS, et al. (2005) 2H-NMR study and molecular dynamics simulation of the location, alignment, and mobility of pyrene in POPC bilayers. *Biophys J* 88: 1818–1827.
25. do Canto AMTM, Santos PD, Martins J, et al. (2015) Behavior of pyrene as a polarity probe in palmitoylsphingomyelin and palmitoylsphingomyelin/cholesterol bilayers : A molecular dynamics simulation study. *Colloid Surface A* 480: 296–306.
26. Kopeć W, Telenius J, Khandelia H, et al. (2013) Molecular dynamics simulations of the interactions of medicinal plant extracts and drugs with lipid bilayer membranes. *FEBS J* 280: 2785–2805.
27. Luch A (2005) *The Carcinogenic Effects of Polycyclic Aromatic Hydrocarbons*, 1Eds., London: Imperial college press.
28. Simons K, Ikonen E (1997) Functional rafts in cell membranes. *Nature* 387: 569–572.
29. Pike LJ (2006) Rafts defined: a report on the Keystone symposium on lipid rafts and cell function. *J Lipid Res* 47: 1597–1598.
30. Veatch SL, Keller SL (2003) Separation of liquid phases in giant vesicles of ternary mixtures of phospholipids and cholesterol. *Biophys J* 85: 3074–3083.
31. Kahya N, Scherfeld D, Bacia K, et al. (2003) Probing lipid mobility of raft-exhibiting model membranes by fluorescence correlation spectroscopy. *J Biol Chem* 278: 28109–28115.
32. Schroeder R, London E, Brown D (1994) Interactions between saturated acyl chains confer detergent resistance on lipids and glycosylphosphatidylinositol (GPI)-anchored proteins: GPI-anchored proteins in liposomes and cells show similar behavior. *Proc Natl Acad Sci* 91: 12130–12134.
33. Ahmed S, Brown D, London E (1997) On the origin of sphingolipid/cholesterol-rich detergent-insoluble cell membranes: physiological concentrations of cholesterol and sphingolipid induce formation of a detergent-insoluble, liquid-ordered lipid phase in model membranes. *Biochemistry* 36: 10944–10953.
34. Schroeder RJ, Ahmed SN, Zhu Y, et al. (1998) Cholesterol and sphingolipid enhance the Triton X-100 insolubility of glycosylphosphatidylinositol-anchored proteins by promoting the formation of detergent-insoluble ordered membrane domains. *J Biol Chem* 273: 1150–1157.
35. Rinia HA, Snel MM, Van der EJP, et al. (2001) Imaging domains in model membranes with atomic force microscopy. *FEBS Lett* 501: 92–96.
36. Klose C, Ejsing CS, Garcá-Sáez AJ, et al. (2010) Yeast lipids can phase-separate into micrometer-scale membrane domains. *J Biol Chem* 285: 30224–30232.
37. Kaiser H, Lingwood D, Levental I, et al. (2009) Order of lipid phases in model and plasma membranes. *Proc Natl Acad Sci* 106: 16645–16650.

38. Sezgin E, Kaiser HJ, Baumgart T, et al. (2012) Elucidating membrane structure and protein behavior using giant plasma membrane vesicles. *Nat Protoc* 7: 1042–1051.
39. Baumgart T, Hammond AT, Sengupta P, et al. (2007) Large-scale fluid/fluid phase separation of proteins and lipids in giant plasma membrane vesicles. *Proc Natl Acad Sci* 104: 3165–3170.
40. Leung SSW, Thewalt J (2017) Link between fluorescent probe partitioning and molecular order of liquid ordered-liquid disordered membranes. *J Phys Chem B* 121: 1176–1185.
41. Barnoud J, Rossi G, Marrink S, et al. (2014) Hydrophobic compounds reshape membrane domains. *PLoS Comput Biol* 10: e1003873.
42. Van Duyl BY, Rijkers DTS, De KB, et al. (2002) Influence of hydrophobic mismatch and palmitoylation on the association of transmembrane α-helical peptides with detergent-resistant membranes. *FEBS Lett* 523: 79–84.
43. Veatch SL, Leung SSW, Hancock REW, et al. (2007) Fluorescent probes alter miscibility phase boundaries in ternary vesicles. *J Phys Chem B* 111: 502–504.
44. Skaug MJ, Longo ML, Faller R (2011) The impact of texas red on lipid bilayer properties. *J Phys Chem B* 115: 8500–8505.
45. Bouvrais H, Pott T, Bagatolli LA, et al. (2010) Impact of membrane-anchored fluorescent probes on the mechanical properties of lipid bilayers. *BBA-Biomembranes* 1798: 1333–1337.
46. Van Duyl BY, Ganchev D, Chupin V, et al. (2003) Sphingomyelin is much more effective than saturated phosphatidylcholine in excluding unsaturated phosphatidylcholine from domains formed with cholesterol. *FEBS Lett* 547: 101–106.
47. Lönnfors M, Doux JPF, Killian JA, et al. (2011) Sterols have higher affinity for sphingomyelin than for phosphatidylcholine bilayers even at equal Acyl-chain order. *Biophys J* 100: 2633–2641.
48. Fritzsching KJ, Kim J, Holland GP (2013) Probing lipid-cholesterol interactions in DOPC/eSM/Chol and DOPC/DPPC/Chol model lipid rafts with DSC and 13C solid-state NMR. *BBA-Biomembranes* 1828: 1889–1898.
49. Engberg O, Yasuda T, Hautala V, et al. (2016) Lipid interactions and organization in complex bilayer membranes. *Biophys J* 110: 1563–1573.
50. Loura LMS, Do Canto AMTM, Martins J (2013) Sensing hydration and behavior of pyrene in POPC and POPC/cholesterol bilayers: A molecular dynamics study. *BBA-Biomembranes* 1828: 1094–1101.
51. Vist MR, Davis JH (1990) Phase equilibria of cholesterol/dipalmitoylphosphatidylcholine mixtures: deuterium nuclear magnetic resonance and differential scanning calorimetry. *Biochemistry* 29: 451–464.
52. Baumgart T, Hunt G, Farkas ER, et al. (2007) Fluorescence probe partitioning between Lo membranes /Ld phases in lipid. *BBA-Biomembranes* 1768: 2182–2194.
53. Juhasz J, Davis JH, Sharom FJ (2010) Fluorescent probe partitioning in giant unilamellar vesicles of 'lipid raft' mixtures. *Biochem J* 430: 415–423.
54. Baumgart T, Hess ST, Webb WW (2003) Imaging coexisting fluid domains in biomembrane models coupling curvature and line tension. *Nature* 425: 821–824.
55. Ramstedt B, Slotte JP (2006) Sphingolipids and the formation of sterol-enriched ordered membrane domains. *BBA-Biomembranes* 1758: 1945–1956.
56. Engelke M, Tähti H, Vaalavirta L (1996) Perturbation of artificial and biological membranes by organic compounds of aliphatic, alicyclic and aromatic structure. *Toxicol In Vitro* 10: 111–115.

57. Cheng T, Zhao Y, Li X, et al. (2012) Computation of octanol-water partition coefficients by guiding an additive model with knowledge. *J Chem Inf Model* 47: 2140–2148.